

Finite-barrier correction for the ferromagnetic resonance frequency of nanomagnets with various magnetocrystalline anisotropies

Yuri P. Kalmykov,¹ Serguey V. Titov,^{2,3} William T. Coffey,³ and William J. Dowling³

¹*Laboratoire de Mathématiques et Physique (EA 4217), Université de Perpignan Via Domitia, F-66860 Perpignan, France*

²*Kotel'nikov Institute of Radio Engineering and Electronics of the Russian Academy of Sciences, Vvedenskii Square 1, Fryazino, Moscow Region 141190, Russia*

³*Department of Electronic and Electrical Engineering, Trinity College, Dublin 2, Ireland*



(Received 15 April 2018; revised manuscript received 30 May 2018; published 18 June 2018)

Finite-barrier corrections to the ferromagnetic resonance (FMR) frequency of nanomagnets are obtained in closed integral form from the undamped *deterministic* equation of motion of the magnetization by averaging the precession frequency as expressed by elliptic functions over all possible precessional trajectories inside a well. The method is illustrated by determining the FMR frequency for nanomagnets with both uniaxial and biaxial anisotropy subjected to a uniform external field and for nanomagnets with *mixed* cubic and uniaxial anisotropy. The results agree with exact numerical calculations obtained from the magnetic Langevin equation via matrix continued fractions.

DOI: [10.1103/PhysRevB.97.224418](https://doi.org/10.1103/PhysRevB.97.224418)

I. INTRODUCTION

A single-domain ferromagnetic nanoparticle is characterized by an internal magnetocrystalline anisotropy potential, having several local states of equilibrium separated by potential barriers between them. If the particle is small (~ 100 Å) so that the potential barriers are relatively low, the magnetization vector \mathbf{M} may cross over the barriers between one potential well and another and vice versa due to thermal agitation. The ensuing thermal instability of the magnetization results in superparamagnetism [1], so prompting Brown [2] to formulate a rigorous treatment of thermal fluctuations in nanoscale ferromagnets rooted in the general theory of stochastic processes. Thus Brown proceeded by taking Gilbert's equation for the motion of \mathbf{M} augmented by a random magnetic field $\mathbf{h}(t)$ with Gaussian white noise properties which may be written in standard Langevin form where the effect of damping and fluctuations is represented by $\gamma\mathbf{h}(t) - \alpha\dot{\mathbf{u}}(t)$ [2], viz.,

$$\dot{\mathbf{u}}(t) = -\{\mathbf{u}(t) \times [\gamma\mathbf{H}(t) + \gamma\mathbf{h}(t) - \alpha\dot{\mathbf{u}}(t)]\}. \quad (1)$$

Here $\mathbf{u} = \mathbf{M}/M_S$ is the unit vector directed along \mathbf{M} , M_S is the saturation magnetization, γ is the gyromagnetic ratio, α is the dimensionless damping parameter, $\mathbf{H} = -(\mu_0 M_S)^{-1} \nabla V$ is the effective magnetic field comprising the anisotropy and external fields, $\mu_0 = 4\pi \times 10^{-7} \text{ JA}^{-2} \text{ m}^{-1}$ in SI units, the operator $\nabla = \partial/\partial\mathbf{u}$ indicates the gradient on the surface of the unit sphere, $V(\vartheta, \varphi)$ is the free-energy density, and the angles ϑ and φ specify the orientation of \mathbf{M} in spherical polar coordinates. Brown [2] then was able to construct from the *magnetic Langevin* equation (1) the accompanying Fokker-Planck equation for the distribution function $W(\vartheta, \varphi, t)$ of the magnetization orientations in configuration space. We remark that although Brown's coherent rotation or "macrospin" approximation cannot completely explain the magnetization dynamics of nanomagnets, nevertheless many qualitative

features needed to explain experimental data are satisfactorily reproduced.

Consequently, many varied problems in superparamagnetism have been analyzed via Brown's model (for reviews, see Refs. [3–5]). In particular, thermal fluctuations strongly affect the ferromagnetic resonance (FMR) in nanomagnets (see, e.g., Refs. [6–10]). However, only a few treatments of FMR in nanomagnets exist. The first one is from Berger *et al.* [6,7], who interpreted FMR spectra via the usual Landau-Lifschitz formula [8] (which ignores thermal fluctuations) with a modified anisotropy constant and saturation magnetization. A similar method was suggested by de Biasi *et al.* [9–11] who modified the well-known Smit-Beljers-Suhl formula for the precession frequency ω_A , viz. [12–14],

$$\omega_A = \frac{\gamma}{\mu_0 M_S \sin \vartheta} \sqrt{\partial_{\vartheta\vartheta} V \partial_{\varphi\varphi} V - (\partial_{\vartheta\varphi} V)^2} \Big|_{\substack{\vartheta=\vartheta_A \\ \varphi=\varphi_A}} \quad (2)$$

(where φ_A, ϑ_A are the angular coordinates of the minimum A of the free-energy density), with suitably adapted anisotropy constant and saturation magnetization. Furthermore, Noginova *et al.* [15,16] calculated the FMR absorption spectra of nanomagnets in the manner of paramagnetic resonance theory, i.e., as a superposition of transitions between all allowed states. The FMR in an assembly of noninteracting magnetic nanoparticles was also studied by Sukhov *et al.* [17], Raikher *et al.* [18–21], and Kalmykov and Coffey [22] using Brown's model based on numerical and analytical methods of solution of Eq. (1).

Now to evaluate the characteristic FMR frequency of a nanomagnet, i.e., the salient parameter of the problem, we consider a magnetic dipole placed in a potential well created by the magnetocrystalline anisotropy $V(\vartheta, \varphi)$. Moreover, we use the fact that for very low damping ($\alpha < 0.01$), where the energy loss per cycle (due to Brownian motion) of a precessing magnetization is very much less than the thermal energy, the energy trajectories diffuse very slowly; therefore they differ,

but little from those of the undamped precessional motion in a well. In other words the dynamics of the magnetization in a well of the potential $V(\vartheta, \varphi)$ are *effectively deterministic* for the purpose of calculating the FMR frequency and in consequence are described by Eq. (1) without damping and noise; i.e., they are simply governed by the deterministic Larmor-like equation,

$$\dot{\mathbf{u}}(t) = \gamma [\mathbf{H}(t) \times \mathbf{u}(t)]. \quad (3)$$

Now the FMR frequency Ω_r can be approximately calculated as the bottom precession frequency ω_A at the bottom of the *deepest* potential well, which is given by Eq. (2). This equation allows one to accurately estimate Ω_r in the zero-temperature limit, $T \rightarrow 0$, corresponding to effectively infinite potential barriers between the metastable states. Unfortunately, Eq. (2) leads to substantial errors in Ω_r for *shallow* potential wells with *relatively small* potential barriers ($\sim 3\text{--}5 kT$). Moreover, Eq. (2) cannot be used for anisotropies with *flat* potential wells, where the factor $\sqrt{\partial_{\vartheta\vartheta} V \partial_{\varphi\varphi} V - (\partial_{\vartheta\varphi} V)^2}$ is exactly equal to zero, because the paraboloidal approximation for V in the vicinity of the minimum A , which is used in the derivation of Eq. (2), is no longer valid. In such cases, the precession frequency of the magnetization depends (in typical nonlinear fashion) on the energy of the magnetic moment, which we can write in nondimensional form as $E(\vartheta, \varphi) = vV(\vartheta, \varphi)/(kT)$, where v is the volume of the nanoparticle, k is Boltzmann's constant, and T is the temperature. The distribution of energy in the well is given by the Boltzmann law $Z_A^{-1} e^{-E(\vartheta, \varphi)}$, where

$$Z_A = \iint_{E < E_C} e^{-E(\vartheta, \varphi)} \sin \vartheta d\vartheta d\varphi$$

is the well partition function and $E_C = vV(\vartheta_C, \varphi_C)/(kT)$ is a saddle (barrier) point energy. The precession frequency $\omega_E = 2\pi P_E^{-1}$ is obtained from the precession period P_E at a given E and so is determined by the line integral [23],

$$P_E = \gamma^{-1} \oint_E |[\mathbf{H} \times \mathbf{M}]|^{-2} ([\mathbf{H} \times \mathbf{M}] \cdot d\mathbf{M}), \quad (4)$$

which in the spherical polar coordinate system becomes

$$P_E = \frac{\mu_0 M_S}{\gamma} \oint_E \frac{\sin \vartheta \frac{\partial V}{\partial \vartheta} d\varphi - \frac{1}{\sin \vartheta} \frac{\partial V}{\partial \varphi} d\vartheta}{\frac{1}{\sin^2 \vartheta} \left(\frac{\partial V}{\partial \varphi}\right)^2 + \left(\frac{\partial V}{\partial \vartheta}\right)^2}. \quad (5)$$

At the bottom of the well [at energy $E_A = vV(\vartheta_A, \varphi_A)/(kT)$], the precession frequency which is now $\omega_A \equiv 2\pi P_{E_A}^{-1}$ reduces to Eq. (2) in the paraboloidal approximation. In writing the general Eqs. (4) and (5), it is assumed [23–25] that one may parametrize the instantaneous magnetization direction by the *slow* energy variable E and the *fast* precessional variable running uniformly along a closed Stoner-Wohlfarth orbit [26] of energy E . Thus, only the purely gyromagnetic term without damping and noise torques need be considered in Eq. (1) (see Refs. [23–25] for details). In thermal equilibrium, the FMR frequency Ω_r of a nanoparticle may be estimated from the energy-dependent precession frequency ω_E of the magnetization vector in the well as averaged over *all possible precessional trajectories* inside the well so that

$$\Omega_r = \frac{1}{Z_A} \iint_{E < E_C} \omega_E(\vartheta, \varphi) e^{-E(\vartheta, \varphi)} \sin \vartheta d\vartheta d\varphi. \quad (6)$$

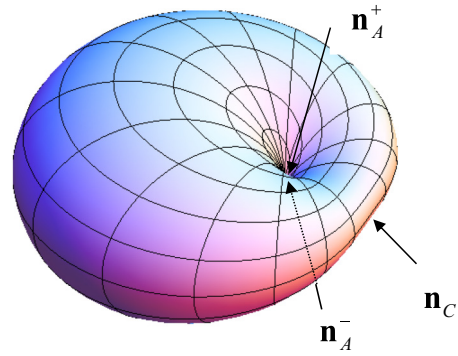


FIG. 1. 3D plot of the dimensionless free energy $E(\vartheta, \varphi)/\sigma$, Eq. (7), for $h = 0.5$.

The integral in Eq. (6) is calculated via the precession period P_E , Eq. (4), along the lossless energy trajectories, i.e., the Stoner-Wohlfarth orbits. Now in certain cases (low potential barriers or flat wells), Ω_r may considerably differ from the bottom precession frequency, Eq. (2).

Therefore, we use Eq. (6) here in order to evaluate the effects of thermal fluctuations on the FMR frequency of nanomagnets with uniaxial, biaxial, and mixed (cubic + uniaxial) anisotropies. The accuracy of the results for Ω_r as obtained from Eq. (6) is ascertained for these potentials by comparing them with independent calculations of the FMR frequency from the spectra of the transverse component of the dynamic susceptibility tensor of a nanoparticle via numerical solution of the magnetic Langevin equation (1) based on the matrix continued fraction method ([5], Chap. 9; see also Appendix A).

II. FMR FREQUENCY FOR UNIAXIAL ANISOTROPY WITH A TRANSVERSE MAGNETIC FIELD

First, we determine the FMR frequency for a uniaxial nanomagnet subject to a uniform dc magnetic field \mathbf{H}_0 applied perpendicular to the easy axis, therefore characterised by the dimensionless free energy

$$E(\vartheta, \varphi) = \sigma(\sin^2 \vartheta - 2h \sin \vartheta \cos \varphi), \quad (7)$$

where $\sigma = vK_u/(kT)$ is the dimensionless anisotropy (inverse temperature) parameter, K_u is the uniaxial anisotropy constant, and $h = \mu_0 M_S H_0 / (2K_u)$ is the external field parameter. The potential Eq. (7) has two *equivalent* wells with minima $E_A = -\sigma h^2$ at \mathbf{n}_A^+ and \mathbf{n}_A^- separated by a potential barrier $\Delta E = E_C - E_A = \sigma(1 - h)^2$ with a saddle point at $E_C = \sigma(1 - 2h)$ at \mathbf{n}_C (see Fig. 1). The saddle point lies in the equatorial region, while \mathbf{n}_A^+ and \mathbf{n}_A^- lie in the north and south polar regions, respectively. In general, $E(\vartheta, \varphi)$ from Eq. (7) retains its *bistable* form for $0 \leq h < h_c$, where $h_c = 1$ is the critical value of h , where $E(\vartheta, \varphi)$ loses its bistable character. The details of the numerical treatment of the problem have been given by Coffey *et al.* [5,27,28], Kennedy [29], Kalmykov and Titov [30], and Fukushima *et al.* [31,32]. Furthermore the nonaxially symmetric double well potential, Eq. (7), is very useful as an illustrative example of how Ω_r may be calculated from Eq. (4).

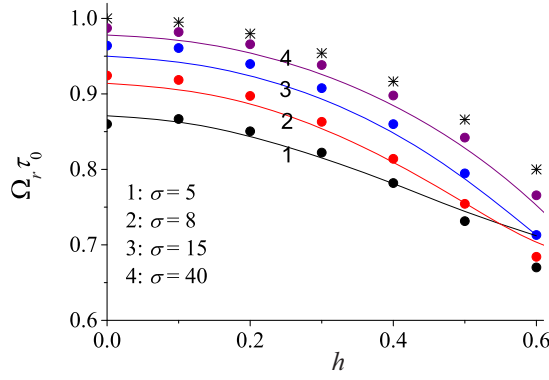


FIG. 2. FMR frequency Ω_r vs the dc field parameter h for various anisotropy (inverse temperature) parameters $\sigma = vK_u/(kT)$. Solid line: continued fraction solution [22]; filled circles: averaged precession frequency Eq. (6); stars: precession frequency at the bottom of the well [Eq. (13)].

Now for $E(\vartheta, \varphi)$ as given by Eq. (7), the Larmor-like gyromagnetic Eq. (3) can be rewritten in terms of the Cartesian components (u_x, u_y, u_z) of the unit vector $\mathbf{u} = \mathbf{M}/M_S$ as

$$\tau_0 \frac{d}{dt} \begin{pmatrix} u_x \\ u_y \\ u_z \end{pmatrix} = \begin{pmatrix} -u_z(t)u_y(t) \\ u_z(t)(u_x(t) - h) \\ hu_y(t) \end{pmatrix}, \quad (8)$$

where

$$\tau_0 = \frac{\mu_0 M_S}{2\gamma K_u} \quad (9)$$

is a precession time constant. For $\gamma = 2.2 \times 10^5 \text{ mA}^{-1} \text{ s}^{-1}$, $M_S \approx 1.4 \times 10^6 \text{ A m}^{-1}$, and $K_u \approx 2 \times 10^5 \text{ J m}^{-3}$ (cobalt), we have the estimate $\tau_0 \approx 2 \times 10^{-11} \text{ s}$.

Furthermore, the line integral Eq. (4) can also be rewritten explicitly in terms of the Cartesian components (u_x, u_y, u_z) as

$$P_E = \oint_E \frac{\dot{u}_x du_x + \dot{u}_y du_y + \dot{u}_z du_z}{\dot{u}_x^2 + \dot{u}_y^2 + \dot{u}_z^2}. \quad (10)$$

Here (u_x, u_y, u_z) are obviously given by the *deterministic* gyromagnetic equation of motion of the magnetization, Eq. (8). Thus, as shown in Appendix B, the periodic time of the magnetization precession, Eq. (10), takes on the final explicit form

$$P_E = \frac{8\tau_0 K(m_E)}{p_E \sqrt{(e_1 - e_3)(e_2 - e_4)}}, \quad (11)$$

where $K(m)$ is the complete elliptic integral of the first kind [33,34] and the parameters p_E, e_1, e_3, e_2, e_4 , and m_E are given in Appendix B by Eqs. (B2), (B9), and (B11), respectively. In the *particular* case of zero external field, $h = 0$, Eq. (11) becomes

$$P_E = \frac{2\pi\tau_0}{\sqrt{1 - E/\sigma}}. \quad (12)$$

The *averaged* precession frequency Ω_r , Eq. (6), as a function of the dc field parameter h is shown in Fig. 2 for various parameters $\sigma = vK_u/(kT)$. Here Ω_r as determined from Eq. (6) is compared with independent calculations of the FMR frequency from the FMR absorption spectra via numerical solution of the magnetic Langevin equation (1) (for details, see [5,21]). Figure 2 shows that Eqs. (6) and (11) used in combination yield an accurate solution for the FMR frequency both at high ($\sigma < 10$) and low ($\sigma < 25$) temperatures for a wide range of the external dc field. Moreover, for large σ , i.e., high barriers (low temperatures), the FMR frequency Ω_r is accurately approximated by the precession frequency ω_A at the bottom of the well, namely,

$$\omega_A = \frac{1}{\tau_0} \sqrt{1 - h^2}. \quad (13)$$

The latter result is obtained by directly substituting the free energy given by Eq. (7) into that given by the parabolic approximation, Eq. (2). Thus, Fig. 2 clearly illustrates that for low barriers, $\Delta E < 5$ (small particles and/or high temperatures), the effect of thermal fluctuations on the FMR frequency may exceed 10%.

III. FMR FREQUENCY FOR BIAxIAL ANISOTROPY

Next, we consider a biaxial anisotropy potential as augmented by the Zeeman term due to an external magnetic field \mathbf{H}_0 . The dimensionless free-energy density $E(\vartheta, \varphi)$ of magnetic nanoparticles taken in standard form including the dc bias field \mathbf{H}_0 is then [5,35]

$$E(\vartheta, \varphi) = \sigma [\delta \sin^2 \vartheta \cos^2 \varphi - \cos^2 \vartheta - 2h(\gamma_3 \cos \vartheta + \gamma_1 \sin \vartheta \cos \varphi + \gamma_2 \sin \vartheta \sin \varphi)], \quad (14)$$

where $\sigma = vK_u/(kT)$ is the dimensionless anisotropy parameter, K_u is the anisotropy constant, δ is the dimensionless biaxiality parameter accounting for both the magnetizing and magnetocrystalline effects, $\gamma_1, \gamma_2, \gamma_3$ are the direction cosines of the field vector \mathbf{H}_0 , and $h = \mu_0 M_S H_0 / (2K_u)$ is as before the external field parameter. We remark that biaxial anisotropy may yield an appreciable contribution to the free-energy density of magnetic nanoparticles [5]. In particular, the bistable potential

TABLE I. The bottom precession frequency.

Potential	Position of minimum	Bottom precession frequency ω_A
$\gamma_3 = 1, \gamma_1 = \gamma_2 = 0$	$\vartheta_A = 0$ and $\vartheta_A = \pi$	$\tau_0^{-1} \sqrt{(1+h)(1+h+\delta)}$
$\gamma_1 = 1, \gamma_2 = \gamma_3 = 0$	$\varphi_A = 0$ and $\sin \vartheta_A = \pm \frac{h}{1+\delta}$	$\tau_0^{-1} \sqrt{1 + \delta - \frac{h^2}{1+\delta}}$
$\gamma_2 = 1, \gamma_1 = \gamma_3 = 0$	$\varphi_A = \pi/2$ and $\sin \vartheta_A = \pm h$	$\tau_0^{-1} \sqrt{(1-h^2)(1+\delta)}$

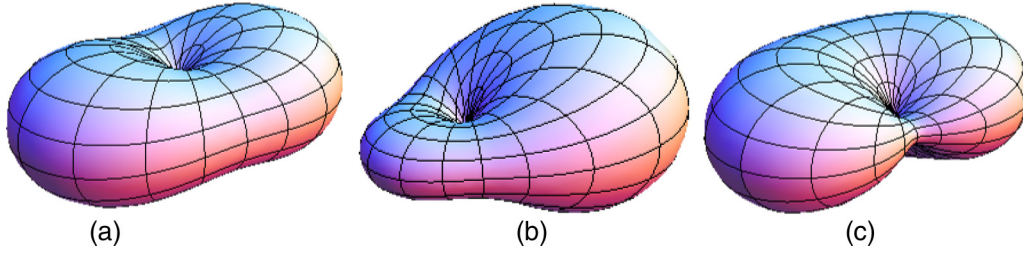


FIG. 3. 3D plots of $\sigma^{-1}E(\vartheta, \varphi)$ (a) Eq. (16), (b) Eq. (18), and (c) Eq. (17) for $\delta = 0.6$ and $h = 0.3$.

is used to describe the free-energy density of a spheroidal nanoparticle, with the axis of symmetry inclined at a certain angle to the easy anisotropy axis of the particle as well that of elongated particles, where easy- and hard-axis anisotropy terms are present [5]. Furthermore, the bistable potential is commonly used in spintronic applications [5,36] to represent the free-energy density of a nanopillar in the standard form of superimposed easy-plane and in-plane easy axis anisotropies.

For the biaxial anisotropy potential, Eq. (14), the gyromagnetic equation, Eq. (3), can again be written for the Cartesian components (u_X, u_Y, u_Z) of the unit vector $\mathbf{u} = \mathbf{M}/M_S$ as a system of differential equations:

$$\tau_0 \frac{d}{dt} \begin{pmatrix} u_X \\ u_Y \\ u_Z \end{pmatrix} = \begin{pmatrix} -u_Y u_Z - h\gamma_3 u_Y + h\gamma_2 u_Z \\ (1 + \delta)u_Z u_X - h\gamma_1 u_Z + h\gamma_3 u_X \\ -\delta u_X u_Y - h\gamma_2 u_X + h\gamma_1 u_Y \end{pmatrix}. \quad (15)$$

We consider now three separate cases. These are where the external magnetic field is applied along the easy axis of magnetization [case (a): $\mathbf{H}_0 \parallel Z, \gamma_3 = 1, \gamma_1 = \gamma_2 = 0$], along the hard axis of magnetization [case (b): $\mathbf{H}_0 \parallel Y, \gamma_2 = 1, \gamma_1 = \gamma_3 = 0$], and along the intermediate axis of magnetization [case (c): $\mathbf{H}_0 \parallel X, \gamma_1 = 1, \gamma_2 = \gamma_3 = 0$] (see Fig. 3). The free-energy density for each of the three cases becomes

$$(a) \quad E(\vartheta, \varphi) = \sigma(\sin^2 \vartheta + \delta \sin^2 \vartheta \cos^2 \varphi - 2h \cos \vartheta), \quad (16)$$

$$(b) \quad E(\vartheta, \varphi) = \sigma(\sin^2 \vartheta + \delta \sin^2 \vartheta \cos^2 \varphi - 2h \sin \vartheta \cos \varphi), \quad (17)$$

$$(c) \quad E(\vartheta, \varphi) = \sigma(\sin^2 \vartheta + \delta \sin^2 \vartheta \cos^2 \varphi - 2h \sin \vartheta \sin \varphi). \quad (18)$$

The free-energy density $E(\vartheta, \varphi)$ from Eqs. (16) and (17) has two wells [which may be either nonequivalent, Eq. (16), or equivalent, Eqs. (17) and (18)] and one or two equivalent saddle points (see Fig. 3). The oscillation frequencies for the deepest well ω_A , Eq. (2), for each of the three potentials (16) and (17) are given in Table I.

Case $\gamma_3 = 1, \gamma_1 = \gamma_2 = 0$. As shown in Appendix B, the magnetization precession period, Eq. (10), now becomes

$$P_E = \frac{2\tau_0 K(m_E)}{p_E \sqrt{(\delta + 1)(1 + e_+)(1 - e_-)}}, \quad (19)$$

where $K(m)$ is the complete elliptic integral of the first kind [33,34] and the parameters p_E, e_{\pm} , and m_E are given by Eqs. (B15), (B16), and (B19), respectively. The FMR frequency Ω_r as a function of the field parameter h and anisotropy (inverse temperature) parameter $\sigma = vK_u/(kT)$ is

shown in Fig. 4. Here Ω_r as given by Eq. (6) is compared with independent calculations of the FMR frequency from the dynamic susceptibility spectra of the nanoparticle obtained via numerical solution of the magnetic Langevin equation (1) (for details, see [35]). The dependence of the FMR frequency on both the dc field parameter h and the biaxiality parameter δ is shown in Fig. 4. For high barriers, the parabolic approximation solution rendered by Eq. (2) is accurate while the weighted Ω_r from Eq. (19) also yields an accurate solution [see Fig. 4(b)]. However, for low barriers (small particle and/or high temperatures), the effect of thermal fluctuations on the FMR frequency may be substantial [more than 10%; see Fig. 4(a)].

Case $\gamma_2 = 1, \gamma_1 = \gamma_3 = 0$. Here, the energy-dependent period P_E of the magnetization precession, Eq. (10), becomes

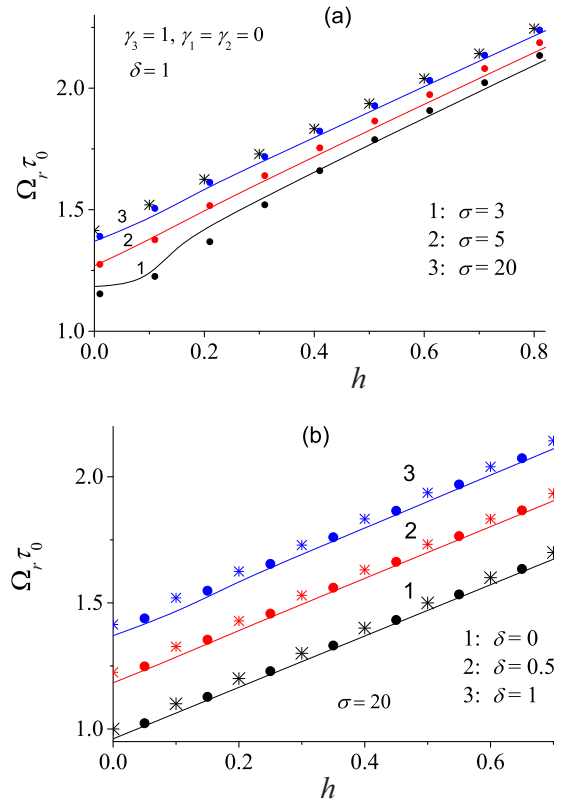


FIG. 4. FMR frequency Ω_r vs the dc field parameter h for $\gamma_3 = 1, \gamma_1 = \gamma_2 = 0$, and various anisotropy parameter values $\sigma = vK_u/(kT)$ (a) and δ (b). Solid line: the FMR frequency calculated via continued fraction solution [35]; filled circles: averaged precession frequency [Eqs. (6) and (19)]; stars: precession frequency at the bottom of the deepest well (see Table I).

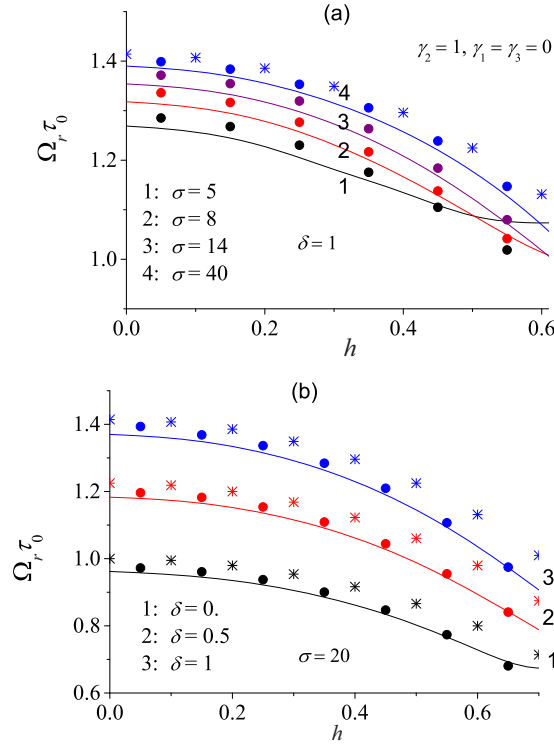


FIG. 5. FMR frequency Ω_r vs the dc field parameter h for $\gamma_2 = 1$, $\gamma_1 = \gamma_3 = 0$, and various anisotropy parameter values σ (a) and δ (b). Solid line: the FMR frequency calculated from the continued fraction solution [35]; filled circles: averaged precession frequency [Eqs. (6) and (20)]; stars: precession frequency at the bottom of the well ω_A from Eq. (2) (see Table I).

(see Appendix B)

$$P_E = \frac{4\tau_0 K(m_E)}{p_E \sqrt{\delta(1+e_+)(1-e_-)}}, \quad (20)$$

where $K(m)$ is the complete elliptic integral of the first kind [33,34] and the parameters p_E, e_{\pm} , and m_E are given by Eqs. (B20), (B24), and (B28), respectively. The FMR frequency Ω_r as a function of the dc field parameter h is shown in Fig. 5. Clearly the small oscillation solution, Eq. (2), is again accurate for high barriers (low temperatures).

Case $\gamma_1 = 1, \gamma_2 = \gamma_3 = 0$. The periodic time, Eq. (10), now becomes (see Appendix B)

$$P_E = \frac{4\tau_0}{p_E \sqrt{\delta}} \left[\frac{K(m_E^{-1})}{\sqrt{2(e_+ - e_-)}} - \frac{K(m_E)}{\sqrt{(1+e_+)(1-e_-)}} \right], \quad (21)$$

where the parameters p_E, e_{\pm} , and m_E are given by Eqs. (B29), (B34), and (B38), respectively. The dependence of the FMR frequency on the dc field parameter h is shown in Fig. 6. Clearly, the small oscillation solution is again accurate at high barriers [Fig. 6(b)]. However, for low barriers (i.e., small particles and high temperatures) the effect of thermal fluctuations on the FMR frequency may be significant [see Fig. 6(a)].

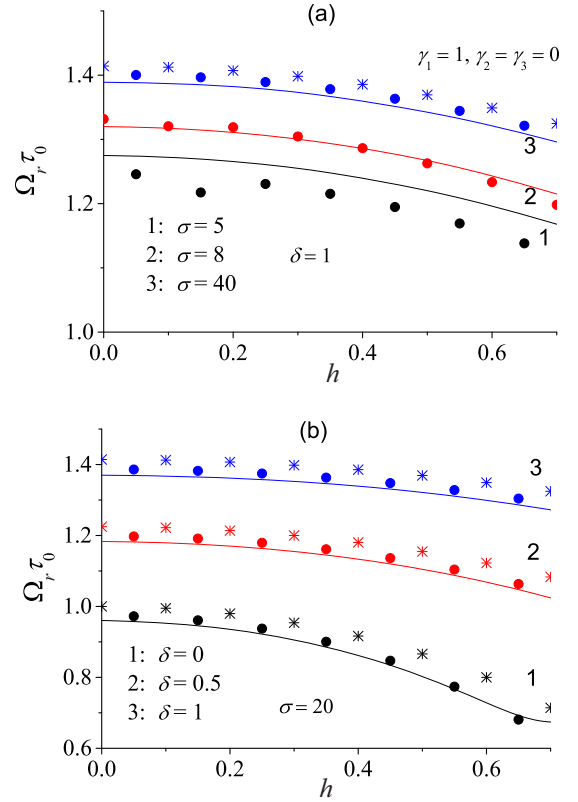


FIG. 6. FMR frequency Ω_r vs the field parameter h for $\gamma_1 = 1$, $\gamma_2 = \gamma_3 = 0$, and various anisotropy parameter values σ (a) and δ (b). Solid line: the FMR frequency calculated via continued fraction solution [35]; filled circles: averaged precession frequency from Eqs. (6) and (21); stars: precession frequency at the bottom of the well ω_A from Eq. (2) (see Table I).

IV. MIXED ANISOTROPY: BREAKDOWN OF THE PARABOLOID APPROXIMATION

The origin of Eq. (2) lies in the paraboloid approximation for the free-energy density $E(\vartheta, \varphi)$ near the bottom of a potential well. However, there are certain situations, where the well frequency ω_A is zero. This obviously incorrect result may occur if the paraboloid approximation fails. The breakdown of that approximation in the well is encountered, for example, for $E(\vartheta, \varphi)$ with flat well bottoms. An example is *mixed* uniaxial and cubic anisotropy [37,38],

$$E(\vartheta, \varphi) = \sigma \left[\sin^2 \vartheta + \frac{\zeta}{4} (\sin^4 \vartheta \sin^2 2\varphi + \sin^2 2\vartheta) \right], \quad (22)$$

where $\sigma = vK_u/(kT)$ is the dimensionless anisotropy parameter, K_u denotes the uniaxial anisotropy constant, and ζ is the cubic-to-uniaxial anisotropy ratio, which may be either positive or negative. For $\zeta = -1$ (see Fig. 7), the anisotropy energy Eq. (22) becomes

$$E(\vartheta, \varphi) = \frac{\sigma}{8} \sin^4 \vartheta (\cos 4\varphi + 7). \quad (23)$$

This value of ζ is of interest, since Eq. (2) cannot now be used to estimate the FMR frequency. Indeed, here the well

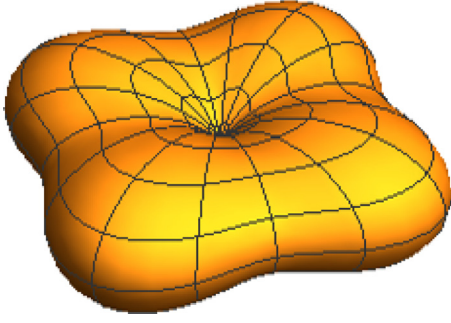


FIG. 7. 3D plots of the mixed anisotropy potential, Eq. (22), for $\zeta = -1$ (flat wells).

frequency is

$$\omega_A = \frac{\gamma}{\mu_0 M_S \sin \vartheta} \sqrt{\partial_{\vartheta\vartheta} V \partial_{\varphi\varphi} V - (\partial_{\vartheta\varphi} V)^2} \Big|_{\substack{\vartheta=\vartheta_{\min} \\ \varphi=\varphi_{\min}}} \equiv 0. \quad (24)$$

For the anisotropy potential, Eq. (22), the gyromagnetic equation (3) can also be written in terms of the Cartesian components (u_x , u_y , u_z) of the unit vector \mathbf{u} as

$$\tau_0 \frac{d}{dt} \begin{pmatrix} u_x \\ u_y \\ u_z \end{pmatrix} = \begin{pmatrix} -u_y u_z (1 - u_z^2 + u_y^2) \\ u_z u_x (1 - u_z^2 + u_x^2) \\ u_x u_y (u_y^2 - u_x^2) \end{pmatrix}. \quad (25)$$

The energy-dependent period, Eq. (10), then becomes (see Appendix B)

$$P_E = 2\tau_0 \int_{e_3}^{e_4} \frac{du}{\sqrt{[(1-u^2)^2 - E/\sigma][4E/\sigma - 3(1-u^2)^2]}}, \quad (26)$$

where the parameters e_3 and e_4 are given by Eq. (B45) in Appendix B. The FMR frequency as a function of the parameter $\sigma = vK_u/(kT)$ is shown in Fig. 8. Clearly the definition of Ω_r via Eq. (6) in combination with the closed Eq. (26), provides a good approximation to the FMR frequency for $\sigma > 10$.

Finally at low potential barriers, $\sigma < 5$, comparison of Ω_r from Eq. (6) with the matrix continued fraction solution

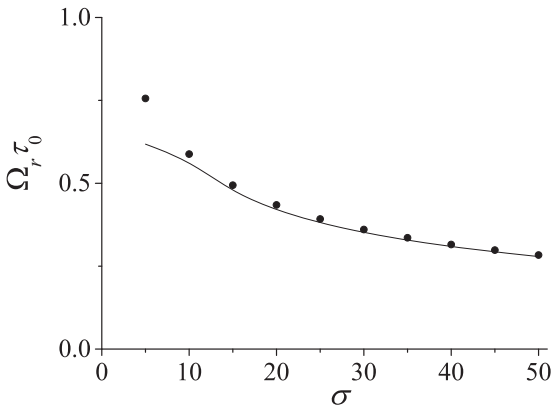


FIG. 8. FMR frequency Ω_r vs the anisotropy (inverse temperature) parameter σ for $\zeta = -1$ (flat wells). Solid line: continued fraction solution [38]; filled circles: averaged precession frequency inside the well Ω_r from Eqs. (6) and (26).

becomes rather complicated as the FMR peak in the spectrum of the imaginary part of the transverse dynamic susceptibility $\chi_{\perp}(\omega)$ then becomes asymmetric and very large due to the inhomogeneous broadening.

V. CONCLUSION

We have evaluated the effects of thermal fluctuations on the *average* FMR frequency of a magnetic nanoparticle for a variety of anisotropy potentials showing that for an acceptable solution all that is actually required is a knowledge of the *deterministic dynamics* governed by the simple gyromagnetic equation and the Boltzmann equilibrium distribution. The calculations clearly illustrate that for low barriers, $\Delta E < 5$ (corresponding to small particles and/or high temperatures), the effect of thermal fluctuations on the FMR frequency may be substantial (more than 10%). In this respect, the determination of the FMR frequency is rather similar to the calculation of the underdamped Kramers' escape rate [4], which is also obtained from the deterministic dynamics of the magnetization. This similarity is unsurprising given that the underdamped escape rate and the FMR frequency are intrinsically linked to each other since they are both aspects of the same phenomenon, namely, the very lightly damped periodic motion in the wells of the magnetocrystalline anisotropy potential. In other words, at low frequencies the effect of the slightly damped librational motion of spins with energy near the barrier energy is to give rise to overbarrier (Néel) relaxation, while at high frequencies the effect of the precessional motion deep in the well is to give rise to ferromagnetic resonance. Moreover, the linking of the frequency resonant process with the low-frequency overbarrier one is yet another example [39] of the original Kramers concept of oscillations in a potential well of Brownian particles with energy equal to the separatrix energy before escape as both are simply limiting cases of the same family of librational dynamical processes in a well. The salient difference between the inertial Brownian motion case pertaining to particles and rigid rotators and the magnetic case is that in the former the low damping process is due to *inertial effects* while in the latter that process arises from geometry.

APPENDIX A: MATRIX CONTINUED FRACTION SOLUTION OF THE MAGNETIC LANGEVIN EQUATION (1)

For *arbitrary* magnetocrystalline anisotropy, which can be written in terms of spherical harmonics $Y_{lm}(\vartheta, \varphi)$ as

$$V(\vartheta, \varphi) = \sum_{R=1}^{\infty} \sum_{S=-R}^R A_{R,S} Y_{RS}(\vartheta, \varphi), \quad (A1)$$

by an appropriate transformation of variables and by direct averaging, the *magnetic Langevin* equation (1) can always be reduced to an infinite hierarchy of differential-recurrence equations for the statistical moments $\langle Y_{lm} \rangle$ (the expectation values of the spherical harmonics), viz. (details are in Ref. [5], Chap. 9),

$$\frac{d}{dt} \langle Y_{lm} \rangle = \sum_{s,r} e_{l,m,l+r,m+s} \langle Y_{l+r,m+s} \rangle, \quad (A2)$$

where $Y_{lm}(\vartheta, \varphi)$ are defined by

$$Y_{lm}(\vartheta, \varphi) = \sqrt{\frac{(2l+1)(l-m)!}{4\pi(l+m)!}} e^{im\varphi} P_l^m(\cos \vartheta),$$

and $P_l^m(x)$ are the associated Legendre functions defined as

$$P_l^m(\cos \vartheta) = \frac{(-1)^m}{2^l l!} (\sin \vartheta)^m \frac{d^{l+m}}{(d \cos \vartheta)^{l+m}} (\cos^2 \vartheta - 1)^l.$$

Furthermore, we can always transform [5] the moment systems, Eq. (A2), into the *tridiagonal* vector differential-recurrence equation

$$\dot{\mathbf{C}}_n(t) = \mathbf{Q}_n^- \mathbf{C}_{n-1}(t) + \mathbf{Q}_n \mathbf{C}_n(t) + \mathbf{Q}_n^+ \mathbf{C}_{n+1}(t) \quad (n > 0), \quad (\text{A3})$$

where $\mathbf{C}_n(t)$ are the column vectors arranged in an appropriate way from the statistical moments $\langle Y_{lm} \rangle(t)$ and the matrices \mathbf{Q}_n^\pm , \mathbf{Q}_n are formed from the elements $e_{l,m,l',m'}$. As shown in Ref. [5], Chap. 9 (see also Refs. [4,28,35,36,38]), Eq. (A3) can then be solved via *matrix continued fractions* for $\langle Y_{10} \rangle(t)$ and $\langle Y_{1\pm 1} \rangle(t)$. Having determined $\langle Y_{10} \rangle(t)$ and $\langle Y_{1\pm 1} \rangle(t)$, we have the Cartesian components of the average magnetization $\langle M_i \rangle(t)$, $i = X, Y, Z$, as

$$\begin{aligned} \langle M_X \rangle(t) &= M_S \sqrt{\frac{2\pi}{3}} [\langle Y_{1-1} \rangle(t) - \langle Y_{11} \rangle(t)], \\ \langle M_Y \rangle(t) &= i M_S \sqrt{\frac{2\pi}{3}} [\langle Y_{1-1} \rangle(t) + \langle Y_{11} \rangle(t)], \\ \langle M_Z \rangle(t) &= M_S \sqrt{\frac{4\pi}{3}} \langle Y_{10} \rangle(t). \end{aligned}$$

In particular, by evaluating the ac stationary response of the magnetization to an ac driving field $H(t) = H \cos \omega t$, we can evaluate the transverse component $\chi_\perp(\omega)$ of the dynamic susceptibility tensor of a nanoparticle, and, hence, the frequency of the FMR peak in the spectrum of the imaginary part of $\chi_\perp(\omega)$ [5]. In practical applications, matrix continued fractions due to their rapid convergence are very well suited to numerical calculations.

APPENDIX B: PERIODS OF THE PRECESSIONAL MOTION FOR VARIOUS ANISOTROPIES

1. Uniaxial nanomagnet subject to a uniform dc magnetic field applied perpendicular to the easy axis

By substituting Eq. (8) into Eq. (10), we have

$$P_E = \tau_0 \oint_E \frac{-u_Z u_Y du_X + (u_Z u_X - h u_Z) du_Y + h u_Y du_Z}{u_Z^2 u_Y^2 + u_Z^2 (u_X - h)^2 + h^2 u_Y^2}. \quad (\text{B1})$$

To calculate this formal integral analytically in terms of elliptic integrals, we rearrange it by using the obvious constraints of energy conservation $E = \text{const.}$ and normalization $|\mathbf{u}| = 1$,

so that

$$1 - E/\sigma = u_Z^2 + 2hu_X = p_E^2 = \text{const.}, \quad (\text{B2})$$

$$u_X^2 + u_Y^2 + u_Z^2 = 1, \quad (\text{B3})$$

where we recall that in the well $-h^2 < E/\sigma < 1 - 2h$, so $p_E^2 > 0$ for $0 < h < h_c = 1$. Next, we introduce a new function $u(t)$ related to $u_X(t)$, $u_Y(t)$, and $u_Z(t)$ via

$$u_X = \frac{p_E^2}{2h} (1 - u^2), \quad (\text{B4})$$

$$u_Y = \sqrt{1 - p_E^2 u^2 - \frac{p_E^4}{4h^2} (1 - u^2)^2}, \quad (\text{B5})$$

$$u_Z = p_E u. \quad (\text{B6})$$

Thus, the line integral, Eq. (B1), can be expressed in terms of the single variable u . Therefore, on substituting Eqs. (B4)–(B6) into Eq. (B1), we simply have the period of the precessional motion in the well,

$$P_E = \frac{2\tau_0}{p_E} \oint_E \frac{du}{\sqrt{\Phi(u)}}, \quad (\text{B7})$$

where

$$\begin{aligned} \Phi(u) &= \frac{4h^2}{p_E^4} - 1 + \left(2 - \frac{4h^2}{p_E^2}\right) u^2 - u^4 \\ &= (e_1 - u)(u - e_2)(u - e_3)(u - e_4) \end{aligned} \quad (\text{B8})$$

and the roots of the fourth-order polynomial $\Phi(u)$ are given by

$$e_{1,2} = -e_{3,4} = \sqrt{1 - \frac{2h^2}{p_E^2} \left(1 \pm \sqrt{1 + \frac{1 - p_E^2}{h^2}}\right)}. \quad (\text{B9})$$

Moreover, $e_1 \leq e_2 \leq e_3 \leq e_4$ for external field parameter values $0 < h < h_c = 1$. Note that in one well u varies in the interval $e_1 \leq u \leq e_2$ while in the other u varies in the interval $e_3 \leq u \leq e_4$ (see Fig. 9). Noticing that

$$\begin{aligned} &\int_{e_3}^{e_4} \frac{dx}{\sqrt{(e_1 - x)(x - e_2)(x - e_3)(x - e_4)}} \\ &= \frac{2K(m_E)}{\sqrt{(e_1 - e_3)(e_2 - e_4)}}, \end{aligned} \quad (\text{B10})$$

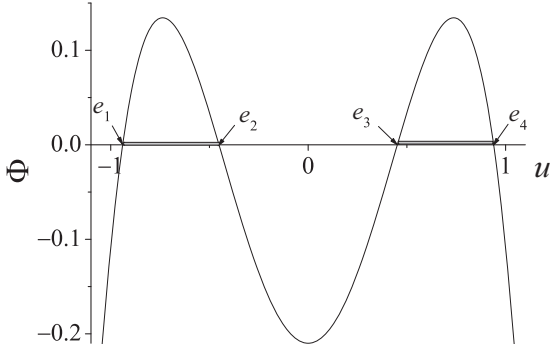
where $K(m)$ is the complete elliptic integral of the first kind [33,34] and the modulus

$$m_E = \frac{(e_1 - e_2)(e_3 - e_4)}{(e_1 - e_3)(e_2 - e_4)}, \quad (\text{B11})$$

we have Eq. (11) for the period of the precessional motion.

2. Biaxial nanomagnet subject to a uniform dc magnetic field

Case $\gamma_3 = 1$, $\gamma_1 = \gamma_2 = 0$. Here, the solutions of Eq. (15) are again subject to the general constraints of energy conservation $E = \text{const.}$ and normalization $|\mathbf{u}| = 1$. The possible value

FIG. 9. The function $\Phi(u)$, Eq. (B8), for $h = 0.4$ and $p_E = 0.95$.

of the normalized free energy of the magnetization in the well is limited by the conditions $E_A \leq E \leq E_C$. If $|h| < h_c = 1$, two nonequivalent wells with minima $E_A = \sigma(-1 \mp 2h)$ at $\vartheta_A = 0, \pi$ and two equivalent saddle points at $E_C = \sigma h^2$ at $\vartheta_C = \pi/2, \varphi_C = \pi/2$ and $\varphi_C = 3\pi/2$ exist [see Fig. 3(a)]. These constraints again allow us to formally introduce a new function $u(t)$ related to $u_X(t)$, $u_Y(t)$, and $u_Z(t)$ via

$$u_X(t) = p_E \sqrt{\delta^{-1}[e_+ - u(t)][e_- - u(t)]}, \quad (\text{B12})$$

$$P_E = \tau_0 \oint_E \frac{[(1+\delta)u_Z + h]u_X du_Y - (u_Y u_Z + h u_Y) du_X - \delta u_X u_Y du_Z}{(u_Z + h)^2 u_Y^2 + \delta^2 u_X^2 u_Y^2 + [(1+\delta)u_Z + h]^2 u_X^2} = -\frac{\tau_0}{p_E \sqrt{\delta+1}} \oint_E \frac{du}{\sqrt{(1-u^2)(u-e_+)(u-e_-)}}. \quad (\text{B17})$$

Thus, we have once again expressed the integrand in terms of the single variable u . Now because

$$\int_{e_-}^{-1} \frac{1}{\sqrt{(1-u^2)(u-e_+)(u-e_-)}} du = -\frac{2}{\sqrt{(1+e_+)(1-e_-)}} K(m_E), \quad (\text{B18})$$

where

$$m_E = \frac{(1+e_-)(1-e_+)}{(1+e_+)(1-e_-)}, \quad (\text{B19})$$

we have for the precessional period, Eq. (19).

Case $\gamma_2 = 1, \gamma_1 = \gamma_3 = 0$. The magnetization trajectories of the precessional dynamics must once again fulfill the two constraints, namely, $|\mathbf{u}| = 1$ and conservation of energy so that

$$p_E^2 = \left(u_Y + \frac{h}{\delta}\right)^2 + \frac{\delta+1}{\delta} u_Z^2 = \frac{\delta+1-E/\sigma}{\delta} + \frac{h^2}{\delta^2} = \text{const.}, \quad (\text{B20})$$

where E is the normalized free energy of the magnetization, with possible values in the well limited by the conditions $E_A \leq E \leq E_C$. If $|h| < h_c = 1$, two equivalent wells exist with minima $E_A = -\sigma h^2$ at $\sin \vartheta_A = \pm h$, $\varphi_A = \pi/2$, and one saddle point at $E_C = \sigma(1-2h)$ at $\vartheta_C = \pi/2, \varphi_C = \pi/2$

$$u_Y(t) = p_E \sqrt{(1+\delta^{-1})[1-u^2(t)]}, \quad (\text{B13})$$

$$u_Z(t) = p_E u(t) - h(\delta+1)^{-1}, \quad (\text{B14})$$

where

$$p_E^2 = \frac{\delta - E/\sigma}{\delta+1} + \frac{h^2}{(\delta+1)^2} = \left[u_Z(t) + \frac{h}{\delta+1}\right]^2 + \frac{\delta}{\delta+1} u_Y^2(t) = \text{const.} \quad (\text{B15})$$

and

$$e_{\pm} = \frac{1}{p_E} \left(-\frac{h\delta}{\delta+1} \pm \sqrt{h^2 - \frac{E}{\sigma}} \right) \quad (\text{B16})$$

are the roots of the quadratic equation $\Phi(u) = 0$, where the polynomial $\Phi(u)$ is explicitly given by

$$\Phi(u) = u^2 + \frac{2\delta h}{p_E(\delta+1)} u + \frac{\delta}{p_E^2} \left[1 - \frac{h^2}{(\delta+1)^2} \right] - \delta - 1.$$

Using Eqs. (B12)–(B16), we have from Eq. (10),

[see Fig. 3(c)]. As before, we can now introduce a new function $u(t)$ related to $u_X(t)$, $u_Y(t)$, and $u_Z(t)$ via

$$u_X(t) = p_E \sqrt{(1+\delta)^{-1}[e_+ - u(t)][u(t) - e_-]}, \quad (\text{B21})$$

$$u_Y(t) = p_E u(t) - \frac{h}{\delta}, \quad (\text{B22})$$

$$u_Z = p_E \sqrt{\frac{\delta}{\delta+1} [1-u^2(t)]}, \quad (\text{B23})$$

where

$$e_{\pm} = \frac{h(\delta+1)}{\delta p_E} \pm \frac{\sqrt{h^2 + E/\sigma}}{p_E} \quad (\text{B24})$$

are the roots of the polynomial

$$\Phi(u) = -\frac{1}{\delta+1} u^2 + 2\frac{h}{p_E \delta} u + \frac{1-h^2/\delta^2}{p_E^2} - \frac{\delta}{\delta+1}. \quad (\text{B25})$$

By substitution of $u_X(t)$, $u_Y(t)$, $u_Z(t)$ given by Eqs. (B21)–(B23) into Eq. (10), we obtain, following our previous method,

$$P_E = \tau_0 \oint_E \frac{(h-u_Y)u_Z du_X + (1+\delta)u_X u_Z du_Y - (\delta u_Y + h)u_X du_Z}{(h-u_Y)^2 u_Z^2 + (1+\delta)^2 u_X^2 u_Z^2 + (\delta u_Y + h)^2 u_X^2} = -\frac{\tau_0}{p_E \sqrt{\delta}} \oint_E \frac{du}{\sqrt{(1-u^2)(e_+ - u)(u - e_-)}}. \quad (\text{B26})$$

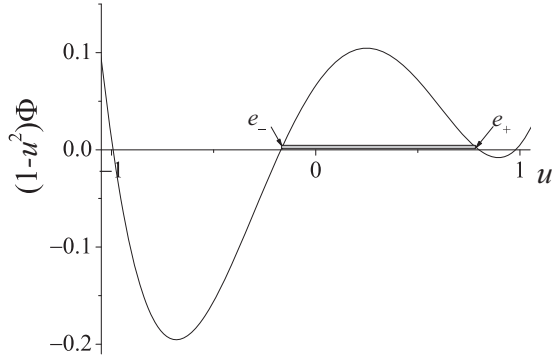


FIG. 10. The function $(1-u^2)\Phi(u)$, Eq. (B25), for $h = 0.2$, $\delta = 1$, and $p_E = 1.3$.

In the well, u varies in the interval $e_- \leq u \leq e_+$ (see Fig. 10). Moreover, the sign of the integral is determined by the direction along the closed trajectory with $E = \text{const}$. Because the integration in interval $e_- \leq u \leq e_+$ corresponds to that over a semiperiod and

$$\int_{e_-}^{e_+} \frac{du}{\sqrt{(1-u^2)(e_+ - u)(u - e_-)}} = \frac{2K(m_E)}{\sqrt{(1+e_+)(1-e_-)}}, \quad (\text{B27})$$

where

$$m_E = \frac{2(e_+ - e_-)}{(1+e_+)(1-e_-)}, \quad (\text{B28})$$

we have Eq. (20) for the precessional period.

Case $\gamma_1 = 1$, $\gamma_2 = \gamma_3 = 0$. The magnetization trajectories of the precessional dynamics must again fulfill the two constraints, namely, $|\mathbf{u}| = 1$ and

$$\begin{aligned} p_E^2 &= \left(u_X - \frac{h}{\delta+1}\right)^2 + \frac{1}{\delta+1}u_Y^2 \\ &= \frac{E/\sigma}{\delta+1} + \frac{h^2}{(\delta+1)^2} = \text{const.}, \end{aligned} \quad (\text{B29})$$

where the possible value of E in the well is limited by the conditions $E_A \leq E \leq E_C$. If $|h| < h_c = 1 + \delta$, we have two equivalent wells with minima $E_A = -\sigma h^2/(1 + \delta)$ at

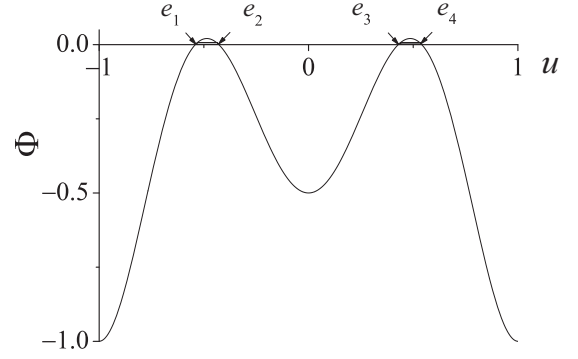


FIG. 11. The function $\Phi(u)$, Eq. (B44), for $E = \sigma/2$.

$\sin \vartheta_A = \pm h/(1 + \delta)$, $\varphi_A = 0$, and saddle points at

$$E_C = \begin{cases} \sigma(1 - h^2/\delta) & h \leq \delta & \vartheta_C = \pi/2, \quad \cos \varphi_C = \pm h/\delta \\ \sigma(1 + \delta - 2h) & \delta \leq h < 1 + \delta & \vartheta_C = \pi/2, \quad \varphi_C = 0 \end{cases} \quad (\text{B30})$$

[see Fig. 3(b)]. Exactly as before, we can introduce a new function $u(t)$ related to $u_X(t)$, $u_Y(t)$, and $u_Z(t)$ via

$$u_X(t) = p_E u(t) + \frac{h}{\delta+1}, \quad (\text{B31})$$

$$u_Y = p_E \sqrt{(\delta+1)[1 - u^2(t)]}, \quad (\text{B32})$$

$$u_Z(t) = p_E \sqrt{(1+\delta)^{-1}[e_+ - u(t)][u(t) - e_-]}, \quad (\text{B33})$$

where

$$e_{\pm} = \frac{h \pm \sqrt{h^2 + \delta(1+\delta)(p_E^2(1+\delta) - 1)}}{p_E(1+\delta)\delta} \quad (\text{B34})$$

are the roots of the polynomial

$$\Phi(u) = \delta u^2 - \frac{2h}{p_E(1+\delta)}u + \frac{1 - h^2/(1+\delta)^2}{p_E^2} - \delta - 1. \quad (\text{B35})$$

By substitution of $u_X(t)$, $u_Y(t)$, $u_Z(t)$ given by Eqs. (B31)–(B33) into Eq. (10), we obtain

$$P_E = \tau_0 \oint_E \frac{-u_Y u_Z du_X + [(1+\delta)u_X - h]u_Z du_Y + (h - \delta u_X)u_Y du_Z}{u_Y^2 u_Z^2 + [(1+\delta)u_X - h]^2 u_Z^2 + (h - \delta u_X)^2 u_Y^2} = -\frac{\tau_0}{p_E \sqrt{(\delta+1)\delta}} \oint_E \frac{du}{\sqrt{(1-u^2)(u-e_+)(u-e_-)}}. \quad (\text{B36})$$

In the well, u varies in the interval $-1 \leq u \leq 1$. Now

$$\int_{-1}^1 \frac{du}{\sqrt{(1-u^2)(u-e_+)(u-e_-)}} = \frac{2K(m_E^{-1})}{\sqrt{2(e_+ - e_-)}} - \frac{2K(m_E)}{\sqrt{(1+e_+)(1-e_-)}}, \quad (\text{B37})$$

where

$$m_E = \frac{2(e_+ - e_-)}{(1+e_+)(1-e_-)}. \quad (\text{B38})$$

Because the integration in interval $-1 \leq u \leq 1$ again corresponds to that over a semiperiod and the sign of the integral is determined by the direction taken along the closed trajectory with $E = \text{const.}$, we have for the precession period, Eq. (21).

3. Mixed anisotropy

For this anisotropy potential, the magnetization trajectories of the precessional dynamics must again fulfill the two constraints, namely, $|\mathbf{u}| = 1$, and

$$p_E^2 = 1 - E/\sigma = u_Z^2 + u_X^2 u_Y^2 + u_X^2 u_Z^2 + u_Y^2 u_Z^2 = \text{const.}, \quad (\text{B39})$$

where $E_A \leq E \leq E_C$. Now two equivalent wells with minima $E_A = 0$ at $\vartheta_A = 0, \pi$ and four saddle points $E_C = 3\sigma/4$ at $\vartheta_C = \pi/2$ and $\varphi_C = \pi n/2, n = 0, 1, 2, 3$ (see Fig. 7) exist. Since

$$u_Y^2 u_X^2 = u_Z^4 - 2u_Z^2 + 1 - E/\sigma$$

and

$$(u_X^2 - u_Y^2)^2 = -3(u_Z^4 - 2u_Z^2 + 1 - 4E/3\sigma),$$

we can therefore again introduce a new function $u(t)$ related to $u_X(t)$, $u_Y(t)$, and $u_Z(t)$ via

$$u_X = \sqrt{\frac{1}{2} \left[1 - u^2 \mp \sqrt{\frac{4E}{\sigma} - 3(1 - u^2)} \right]}, \quad (\text{B40})$$

$$u_Y(t) = \sqrt{\frac{1}{2} \left[1 - u^2 \pm \sqrt{\frac{4E}{\sigma} - 3(1 - u^2)} \right]}, \quad (\text{B41})$$

$$u_Z(t) = u(t). \quad (\text{B42})$$

By substituting $u_X(t)$, $u_Y(t)$, $u_Z(t)$ given by Eqs. (B40)–(B42) into Eq. (10), we have

$$\begin{aligned} P_E &= \tau_0 \oint_E \frac{-u_Y u_Z (1 - u_Z^2 + u_Y^2) du_X + u_Z u_X (1 - u_Z^2 + u_X^2) du_Y + u_X u_Y (u_Y^2 - u_X^2) du_Z}{u_Y^2 u_Z^2 (1 - u_Z^2 + u_Y^2)^2 + (1 - u_Z^2 + u_X^2)^2 u_Z^2 u_X^2 + (u_Y^2 - u_X^2)^2 u_X^2 u_Y^2} \\ &= -\tau_0 \oint_E \frac{du}{\sqrt{\Phi(u)}}, \end{aligned} \quad (\text{B43})$$

where

$$\Phi(u) = [(1 - u^2)^2 - E/\sigma][4E/\sigma - 3(1 - u^2)^2], \quad (\text{B44})$$

and u varies in the intervals $e_1 \leq u \leq e_2$ and $e_3 \leq u \leq e_4$ (see Fig. 11), where

$$e_{1,3} = \mp \sqrt{1 - 2\sqrt{\frac{E}{3\sigma}}}, \quad e_{2,4} = \mp \sqrt{1 - \sqrt{\frac{E}{\sigma}}} \quad (\text{B45})$$

are the roots of the polynomial $\Phi(u)$. The sign of the integral is again determined by the direction along the closed trajectory with $E = \text{const.}$ Therefore, we have Eq. (26) for the precession period P_E .

-
- [1] C. P. Bean and J. D. Livingston, Superparamagnetism, *J. Appl. Phys. Suppl.* **30**, 120S (1959).
- [2] W. F. Brown, Jr., Thermal fluctuations of a single-domain particle, *Phys. Rev.* **130**, 1677 (1963); Thermal fluctuations of fine ferromagnetic particles, *IEEE Trans. Magn.* **15**, 1196 (1979).
- [3] J. L. Dormann, D. Fiorani, and E. Tronc, Magnetic relaxation in fine-particle systems, *Adv. Chem. Phys.* **98**, 283 (1997).
- [4] W. T. Coffey and Y. P. Kalmykov, Thermal fluctuations of magnetic nanoparticles: Fifty years after Brown, *J. Appl. Phys.* **112**, 121301 (2012).
- [5] W. T. Coffey and Y. P. Kalmykov, *The Langevin Equation*, 4th ed. (World Scientific, Singapore, 2017).
- [6] R. Berger, J. Kliava, J.-C. Bissey, and V. Baietto, Magnetic resonance of superparamagnetic iron-containing nanoparticles in annealed glass, *J. Appl. Phys.* **87**, 7389 (2000).
- [7] R. Berger, J.-C. Bissey, J. Kliava, H. Daubric, and C. Estournès, Temperature dependence of superparamagnetic resonance of iron oxide nanoparticles, *J. Magn. Magn. Mater.* **234**, 535 (2001).
- [8] L. D. Landau and E. M. Lifshitz, On the theory of the dispersion of the magnetic permeability of ferromagnetic bodies, *Phys. Z. Sowjetunion* **8**, 153 (1935).
- [9] R. S. de Biasi and T. C. Devezas, Anisotropy field of small magnetic particles as measured by resonance, *J. Appl. Phys.* **49**, 2466 (1978).
- [10] E. de Biasi, C. A. Ramos, and R. D. Zysler, Size and anisotropy determination by ferromagnetic resonance in dispersed magnetic nanoparticle systems, *J. Magn. Magn. Mater.* **262**, 235 (2003).
- [11] E. de Biasi, E. Lima, Jr., C. A. Ramos, A. Butera, and R. D. Zysler, Effect of thermal fluctuations in FMR experiments in uniaxial magnetic nanoparticles: Blocked vs. superparamagnetic regimes, *J. Magn. Magn. Mater.* **326**, 138 (2013).
- [12] J. Smit and H. G. Beljers, Ferromagnetic resonance absorption in BaFe₁₂O₁₉ a highly anisotropic crystal, *Philips Res. Rep.* **10**, 113 (1955).
- [13] H. Suhl, Ferromagnetic resonance in nickel ferrite between one and two kilomegacycles, *Phys. Rev.* **97**, 555 (1955).

- [14] G. V. Skrotskii and L. V. Kurbatov, Phenomenological theory of ferromagnetic resonance, in *Ferromagnetic Resonance*, edited by S. V. Vonsovskii (Pergamon Press, Oxford, 1966), Chap. 2, p. 12.
- [15] N. Noginova, F. Chen, T. Weaver, E. P. Giannelis, A. B. Bourlinos, and V. A. Atsarkin, Magnetic resonance in nanoparticles: between ferro- and paramagnetism, *J. Phys.: Condens. Matter* **19**, 246208 (2007).
- [16] N. Noginova, T. Weaver, E. P. Giannelis, A. B. Bourlinos, V. A. Atsarkin, and V. V. Demidov, Observation of multiple quantum transitions in magnetic nanoparticles, *Phys. Rev. B* **77**, 014403 (2008).
- [17] A. Sukhov, K. D. Usadel, and U. Nowak, Ferromagnetic resonance in an ensemble of nanoparticles with randomly distributed anisotropy axes, *J. Magn. Magn. Mater.* **320**, 31 (2008).
- [18] Yu. L. Raikher and M. I. Shliomis, Theory of dispersion of magnetic susceptibility of fine ferromagnetic particles, *Zh. Eksp. Teor. Fiz.* **67**, 1060 (1974) [*Sov. Phys. JETP* **40**, 526 (1975)].
- [19] Yu. L. Raikher and V. I. Stepanov, The effect of thermal fluctuations on the FMR line shape in dispersed ferromagnets, *Zh. Eksp. Teor. Fiz.* **102**, 1409 (1992) [*Sov. Phys. JETP* **75**, 764 (1992)].
- [20] Yu. L. Raikher and V. I. Stepanov, Ferromagnetic resonance in a suspension of single-domain particles, *Phys. Rev. B* **50**, 6250 (1994); Intrinsic magnetic resonance in superparamagnetic systems, **51**, 16428 (1995).
- [21] I. S. Poperechny and Yu. L. Raikher, Ferromagnetic resonance in uniaxial superparamagnetic particles, *Phys. Rev. B* **93**, 014441 (2016); I. S. Poperechny, Yu. L. Raikher, and V. I. Stepanov, Ferromagnetic resonance in a dilute suspension of uniaxial superparamagnetic particles, *J. Magn. Magn. Mater.* **424**, 185 (2017).
- [22] Yu. P. Kalmykov and W. T. Coffey, Transverse complex magnetic susceptibility of single-domain ferromagnetic particles with uniaxial anisotropy subjected to a longitudinal uniform magnetic field, *Phys. Rev. B* **56**, 3325 (1997).
- [23] T. Dunn, A. L. Chudnovskiy, and A. Kamenev, Dynamics of nano-magnetic oscillators, in *Fluctuating Nonlinear Oscillators*, edited by M. Dykman (Oxford University Press, London, 2012).
- [24] W. T. Coffey, Y. P. Kalmykov, and S. V. Titov, Magnetization reversal time of magnetic nanoparticles at very low damping, *Phys. Rev. B* **89**, 054408 (2014).
- [25] D. J. Byrne, W. T. Coffey, W. J. Dowling, Yu. P. Kalmykov, and S. V. Titov, On the Kramers very low damping escape rate for point particles and classical spins, in *Advances in Chemical Physics*, edited by S. A. Rice and A. R. Dinner (Wiley, New York, 2015), Vol. 156, p. 393.
- [26] E. C. Stoner and E. P. Wohlfarth, A mechanism of magnetic hysteresis in heterogeneous alloys, *Philos. Trans. R. Soc. A* **240**, 599 (1948).
- [27] W. T. Coffey, D. S. F. Crothers, J. L. Dormann, L. J. Geoghegan, Yu. P. Kalmykov, J. T. Waldron, and A. W. Wickstead, Effect of an oblique magnetic field on the superparamagnetic relaxation time, *Phys. Rev. B* **52**, 15951 (1995).
- [28] W. T. Coffey, D. S. F. Crothers, Yu. P. Kalmykov, and S. V. Titov, Precessional effects in the linear dynamic susceptibility of uniaxial superparamagnets: Dependence of the ac response on the dissipation parameter, *Phys. Rev. B* **64**, 012411 (2001).
- [29] E. E. C. Kennedy, Relaxation times for single domain ferromagnetic particles, *Adv. Chem. Phys.* **112**, 211 (2000).
- [30] Yu. P. Kalmykov and S. V. Titov, The complex magnetic susceptibility of uniaxial superparamagnetic particles in a high constant magnetic field, *Fiz. Tverd. Tela (S.-Peterburg)* **40**, 1642 (1998) [*Phys. Solid State* **40**, 1492 (1998)].
- [31] H. Fukushima, Y. Uesaka, Y. Nakatani, and N. Hayashi, Switching times of a single-domain particle in a field inclined off the easy axis, *J. Appl. Phys.* **101**, 013901 (2007).
- [32] H. Fukushima, Y. Uesaka, Y. Nakatani, and N. Hayashi, Dependence of prefactor on the angle between an applied field and the easy axis for single-domain particles, *J. Magn. Magn. Mater.* **323**, 195 (2010).
- [33] *Handbook of Mathematical Functions*, edited by M. Abramowitz and I. A. Stegun (Dover, New York, 1972).
- [34] E. T. Whittaker and G. N. Watson, *A Course of Modern Analysis*, 4th ed. (Cambridge University Press, London, 1927).
- [35] B. Ouari, S. V. Titov, H. El Mrabti, and Y. P. Kalmykov, Non-linear susceptibility and dynamic hysteresis loops of magnetic nanoparticles with biaxial anisotropy, *J. Appl. Phys.* **113**, 053903 (2013).
- [36] Yu. P. Kalmykov, W. T. Coffey, S. V. Titov, J. E. Wegrowe, and D. Byrne, Spin-torque effects in thermally assisted magnetization reversal: Method of statistical moments, *Phys. Rev. B* **88**, 144406 (2013).
- [37] A. J. Newell, Superparamagnetic relaxation times for mixed anisotropy and high energy barriers with intermediate to high damping: 2. Uniaxial axis in a (111)direction, *Geochem. Geophys. Geosyst.* **7**, Q03015 (2006); Superparamagnetic relaxation times for mixed anisotropy and high energy barriers with intermediate to high damping: 1. Uniaxial axis in a (001)direction, **7**, Q03016 (2006).
- [38] W. T. Coffey, P. M. Déjardin, and Yu. P. Kalmykov, Reversal time of the magnetization of single-domain ferromagnetic particles with mixed uniaxial and cubic anisotropy, *Phys. Rev. B* **79**, 054401 (2009).
- [39] W. T. Coffey, Yu. P. Kalmykov, S. V. Titov, and D. S. F. Crothers, High-frequency resonance absorption as evidence for oscillation in a well before escape from a metastable state in the Kramers energy diffusion model, in *Recent Advances in Broadband Dielectric Spectroscopy*, edited by Yu. P. Kalmykov, NATO Science for Peace and Security Series B: Physics and Biophysics (Springer, Dordrecht, 2013), Chap.11, p. 151.